Indian Journal of Chemical Technology
Vol. 28, January 2021, pp. 23-35

Enhanced adsorption of fluoride by common potters'clay surface modified by zirconium oxide particles

Paran Jyoti Kalita[1,2] , Jitu Saikia[1] , Susmita Sarmah[1] & Rajib Lochan Goswamee*[,1]

[1]Advanced Materials Group, Materials Science & Technology Division, CSIR-North East Institute of Science & Technology, Jorhat 785 006, India

[2]Department of Chemistry, Gauhati University, Guwahati 781 014, India

E-mail: *goswamirl@neist.res.in*

Received 6 January 2020; accepted 9 September 2020

The present study aims to enhance the fluoride removal capacity of a low cost material common potters' clay by surface modification through oxidic particles. Zirconium oxide particles have been supported over the clay surface to achieve the objective. Results revealed that the adsorbent is very efficient in a wide *p*H range of 3-11.The adsorption process followed a Freundlich isotherm model signifying that the adsorption took place on the surface in a multilayer form. Kinetic study show that adsorption gained equilibrium within 120 min and it follow pseudo 2nd order kinetics. From this study, it is found that fluoride adsorptive power of common potters' clay can be improved through surface modification of the clay by supporting ZrO_2 particles.

Keywords: Adsorption, Fluoride, Kinetics, Potters' clay, Zirconium oxide

Unfettered expansion of pollution of water bodies is making the accessibility of safe drinking water a serious global issue in the present days[1-3]. One such major concern is the contamination of ground water by fluoride ion. Although the presence of Fluoride in water at low concentrations is considered as beneficial from the perspective that it is a vital micronutrient to prevent dental carries and mineralization of hard tissues[4-6] yet exposure to a high level of fluoride in water can lead to severe and chronic ill effects on health[3,7] like softening of bones, ossification of tendons and ligaments, and abnormal bone growth also called as skeletal fluorosis[5,8,9]. It can also cause dental fluorosis, osteoporosis, arthritis, brittle bones, cancer, infertility, brain damage, Alzheimer syndrome, and thyroid disorder[2,3,10]. The World Health Organization has set a guidance limit of 1.5 mg/L[11,12]. However, for tropical countries generally recommended maximum fluoride concentrations are 1.0 mg/L as in these countries the consumption level of water by the people is higher compared to the people in temperate countries[2,13,14]. During the last few decades, fluoride levels in the ground and surface water have increased gradually in numerous underground aquifers and water bodies across the globe[3, 10], resulting in rapid increase of the cases of fluorosis. In countries like India, fluorosis is consistently expanding and the reasons for the same are the expanding population, increasing need of ground water and arbitrary selection of sites for deep well digging, excessive utilization of shallow hand pump for water extraction and poor-quality control measures[15]. In India, 230 areas of 20 states have elevated amounts of fluoride with groundwater concentration of fluoride being more than the permissible limit[15]. In the state of Assam, the main fluoride affected districts are Karbi Anglong, Nagaon, Goalpara, Kamrup (Rural), and Kamrup (Metro) district[16].

Hence, due to the global seriousness of the problem immediate attention is needed to develop technologies which are of low-cost and environmentally benign. Technologies, that could help to minimize the fluoride exposure of human society as a whole and the limit set up by the WHO could be easier to be maintained universally. Presently, there are a wide variety of technology options available in the market for the remediation of the problem of fluoride contamination in drinking water. Some of such most commonly employed defluoridation techniques are ion exchange[17], precipitation[11], electro coagulation[17], catalytic ozonation[5], reverse osmosis[18], membrane filtration[19], nano filtration[20], and adsorption[18,21]. Out of this long list of different available defloridation techniques, adsorption is considered as the most powerful technique. This is due to its advantages of

ease in handling and cost-effectiviness in maintenance[18,21,22]. It has a minimal requirement of instrumentation and the choice of a wide range of specific adsorbent materials. Accordingly, it is considered as most suitable method for the removal of toxic substances like fluoride from water in developing countries like India. Reports of different prominent adsorbent materials utilised against fluoride so far are modified cellulose fiber[23], bone charcoal[24], activated alumina[25], activated carbon[26], hydrotalcite-like compounds[27] and magnetic adsorbents[27]. Despite the presence of so many adsorbents, yet there is a high demand for alternative cost-effective and environment friendly adsorbent for the removal of fluoride from contaminated water.

Natural clay minerals and materials derived from clay are widely used as adsorbent for various water treatment processes. By using these minerals the advantages like lower cost, easy availability, environment friendliness, ease of handling are achieved. Technically, also several type of clay minerals possess important properties that favour higher adsorption, they are high surface area, high ion exchange capability, molecular sieve like structure, chemical stability and variation of surface and structural properties[28]. Especially, with reference to adsorption of Fluoride ion clays have additional advantages as substantial amount of aluminium oxide present in clays makes them good adsorbent[29]. This is because of high electropositive nature of aluminium as a result of which it binds strongly with fluorine through hard-hard interaction as the latter possess a highly electronegative nature[30].

In the present work it was studied whether the adsorptive power of natural clay can be further enhanced chemically by modifying its surface with supported zirconium oxide particles. It is an established fact that when some oxidic particles are supported on a suitable surface they would not only be activated for participation in chemical reactions also the atom efficiency for adsorption can be expected to be enhanced[31]. Enhanced adsorption is one of the key factor for cost advantages also. Presently, zirconium-based sorbents are attracting more attention from the researchers due to their high affinity for fluoride[8] and low toxicity. Zirconium oxides/hydroxides are reported as powerful adsorbent for dyes, uranium (IV), phosphate, mercury, and selenium[32]. Side by side, from the perspectives of human physiological requirement also it is known that the daily dietary intake of zirconium in human is approximately 4.15 milligrams of which 3.5 milligrams should be from food and 0.65 milligrams from water[33]. While, aquatic plant shows some tendency for zirconium adsorption but most of the plants found on land have no such tendency for Zr adsorption[34].

As per our literature survey, the removal of fluoride from aqueous medium by using zirconium oxide loaded natural clay is scanty. Therefore, in our present investigation, we believe we are making one first time report of the preparation of a zirconium oxide loaded natural clay material for its application in the removal of fluoride from aqueous medium.

Experimental Section

Materials

Locally accessible potters' clay was collected from southern region of Golaghat district, Assam, India ($26^{o}36.115$, $93^{o}58.223$) denoted as DKC. Zirconium (IV) oxide chloride was purchased from Avra Synthesis Pvt. Ltd.; NaF was purchased from Merck (Germany). KBr, KCl, Na_2CO_3 and Na_2SO_4 were purchased from HIMEDIA (India).

Preparation of adsorbent

The zirconium oxide activated clay adsorbent was prepared by a method as reported by Chaudhry *et al*.[35]. Firstly; the organic matters from the collected clay were removed by treatment with H_2O_2. Then 2.0 mL of 1 M citric acid solution dissolved in ethanol was added to 250 mL of 0.125 M $ZrOCl_2.8H_2O$ solution. The purpose of addition of citric acid was to act as a capping agent to control the size of zirconium oxide particles in nanoscale sizes. After that the mixture was stirred for 30 min at 323 K temperature on a magnetic stirrer and subsequently 50 g of clay samples was added to the solution. The stirring was done for 10 h at room temperature and then filtered through a Whatman 41 filter paper and resulting clay residue was washed with distilled water for several times to remove loosely bound oxide particles. Finally, the clay residue dried in an air oven at 378 K and collected for subsequent experiment (denoted as ZrO-DKC).

Adsorbent characterisation

Powder X-ray diffraction

The prepared ZrO-DKC adsorbent was chracterised by using powder X-ray diffractrometer (type: Rigaku

UltimaIV).The measurement was set up at starting angle of 2° and stop angle at 75°. Step angle was maintained at 0.05° with a scanning rate of 3° per minute. The source of X-Ray was Cuk_{α} (λ = 1.54056 Å). The diffractrogram was processed by using the program 'XG operation RINT 2200' linked with the powder XRD data station. The peaks were identified by using the library database 'Rigaku PDXL 1.2.0.1'. The standard ICDD (International Centre for Diffraction Data) card was employed to identify different phases.

Scanning Electron Microscope

The electron beam study (SEM) images were taken in Field Emission Scanning Electron Microscopy (FE-SEM) Make Carl Zeiss Germany Model ZEISS Sigma. For SEM analysis the samples were dried in an oven at around 100°C and kept in a vacuum desiccator for two to three times before the SEM analysis. The SEM images were further developed by using ImajJ software.

Brunauer-Emmett-Teller (BET) measurements

The textural properties of the adsorbent mainly specific area, pore volume, and average pore diameter were tested by using an AutosorbiQ Station 1(Make-Quantrachrom), equipped with an automated surface area at 77.35 K using Brunauet-Emmett-Teller (BET) calculation for surface area. Sample outgas temperature was maintained at 250°C.

Thermo gravimetric analysis

The non-isothermal analysis (TGA/DTG) of the sample was conducted in a simultaneous TGA-DTA-DSC thermal analyzer system (Model STA449 F3, Jupiter) in atmosphere of nitrogen. Heating rate was maintained at 10°C min^{-1} from room temperature to 1000°C using a platinum crucible.

X-ray photoelectron spectroscopy measurements

X-ray photoelectron spectroscopy (XPS) measurements were carried out by using an X-ray photoelectron spectrometer (ESCALABXi^{+}, Thermo Fisher Scientific, UK). The X-ray radiation source was monochromatic Al K (1486.74 eV) and the photo excited electrons were analyzed in constant pass energy mode with a pass energy of 50 eV.

Fourier transform infrared (FT-IR) spectra were recorded in a Perkin-Elmer system 2000 (model 640B, software version 4.07) by using KBr pellets.

Zero point charge determination

The zero point charge of ZrO-DKC was determined by using ZETASIZER (Model: Nano ZS, MALVERN, UK) adopting auto-titration method at different *p*H ranging from 3-9.

Adsorption studies

To accomplish adsorption studies at room temperatures 30±1°C, ZrO-DKC was taken in finely ground state. 0.22323 g of NaF was dissolved in 1000 ml double distilled water to prepare 100 mg L^{-1} Fluoride stock solution. Diluting the stock solution, different concentrations like 5.65, 17.9, 19.75, 22.9, 41.6, 49.7,50, 59.5, 81.4, 91.9 mg L^{-1} fluoride solution were prepared. To know the adsorption behaviour of fluoride onto the adsorbent surface, the impacts of various factors like equilibrium dose of adsorbent, equilibrium contact time of the adsorbent, *p*H, temperature, the initial concentration of adsorbates and co-existing anions were examined. The knowledge of impact of adsorbent dose on adsorption is a significant factor to improve a process for determining the optimum adsorption efficiency. To study the impact of adsorbent dose varying amounts of adsorbents were taken in separate Teflon bottles and treated with 20 mL of 18 mg/L fluoride solution. The experiments were carried out at 30°C by shaking the suspensions at 200 rpm in a mechanical shaker for 120 min. The equilibrium time of adsorption was determined by using a constant initial fluoride concentration of 18 mgL^{-1} for different contact times. To investigate the nature of adsorption and spontaneity of F^{-} adsorption on ZrO-DKC, the temperature effect on adsorption was tested at five different temperatures viz. 303 K, 313 K, 323 K, and 333 K using 19.75 mg L^{-1} fluoride solution. The impact of initial fluoride concentration on the adsorption of fluoride by ZrO-DKC at equilibrium time was investigated at a constant adsorbent dose of 0.75 g for 20 mL of fluoride solution of various concentrations such as 91.9, 81.4, 59.5, 49.7, 41.6, 22.9, 20.1, 17.9, and 5.65 mgL^{-1}. Sulphate, chloride, bromide, carbonate, and phosphate are generally occurring anions in water and these anions compete with fluoride ions during adsorption[14]. Batch mode study of the effect of these co-existing anions on adsorption of fluoride was done by evaluating the remaining fluoride concentration in absence of other anions, in presence of each anion and all anions together using 20 mg L^{-1} fluoride solution in the presence of 20 mgL^{-1} anion solutions. The batch mode

study of the impact of *p*H of fluoride solution on defluoridation was done by evaluating the remaining fluoride concentration from initial 29 mg L^{-1}. Fluoride solution maintained at different *p*H from 2.1 to 11. ZrO-DKC was used to study the removal of fluoride from real groundwater collected from Burha pahar area of Nagaon district of Assam. The different chemical parameters of the groundwater were determined by standard method (IS:3025-1964).

Equation 1 and 2 were utilised to calculate adsorption efficiency (E), and adsorption capacity(S) respectively.

$$E = \frac{C_o - C_e}{C_o} X\ 100 \quad \ldots (1)$$

$$S = \frac{C_o - C_e}{W_m} X\ V \quad \ldots (2)$$

Where, C_o and C_e denoted the initial and equilibrium concentration of the F^- ion. W_m and V represent the adsorbent mass (g) and volume (L) of treated adsorbates solution respectively. Orion 4 star (pH/ISE) selective ion electrode was used to measure the residual concentration of fluoride in solution. The electrode was calibrated with 0.1, 1, 10, 100 mgL^{-1} standard fluoride solutions. The ionic strength of the fluoride solution was controlled by Total Ionic Strength Adjustment Buffer (TISAB-III). Critical results were cross checked by using an 881 Compact IC pro Metrohm ion chromatograph (Switzerland) associated with an anion column (MetrosepA Supp 5 250/4.0), at a flow rate of the eluent 0.6 mL/min and a pressure of 12.39 MPa with a recording time of 35.0 min. Where, 3.2 mM Na_2CO_3 + 1.0 mM $NaHCO_3$, H_2SO_4 eluent was used as mobile phase and ultrapure water were used to rinse and maintain the conductivity.

Results and Discussion

Adsorbent characterisation

Powder XRD characterisation

The XRD patterns of the raw clay and ZrO-DKC adsorbent are presented in Fig. 1(A). It is observed that the peaks correspond to DKC are prominent to the preapred composite but there is a slight decrease in peak intensity in the composite. This decrease in intensity may be due to the distortion of native crystal packing by the chemical action over the basal planes of clay surface[35]. The major minerals present in the raw clay samples were found to be kaolinite (K) (ICDD card no 00-001-0527), and quartz (Q) (ICDD card no: 00-003-0419). The different phases in the native as well as ZrO-DKC is listed in Table 1.

TGA characterisation

Figure 1(B) shows the thermal behaviour and stability of the prepared ZrO-DKC material. From the curve, it is found that at a temperature range of 30-200°C, 4.16% mass loss was observed, which is due to the loss of adsorbed water. The mass loss of 6.06% at a temperature range 200-600°C is due to the loss of organic matter. Since, the residual mass is found to be 88.72%, it indicated that the prepared ZrO-DKC is largely thermostable up to 1000°C. Since the thermal stability reflects the crystal-chemical stability of the oxidic framework of the components of the composite adsorbent therefore they may be considered as an indicator of a possible stability of the adsorbent in various physico-chemical conditions.

FTIR spectra

The Fourier transform infrared spectroscopy spectrum of the ZrO-DKC and native DKC is shown in Fig. 1(C). The absorption band at 3628 cm^{-1} and 1633 cm^{-1} is due to the stretching and bending vibration of O-H groups in the crystal and absorbed water molecules, respectively[36]. The presence of absorption band centred at 803 cm^{-1}, is due to Si-O-Si inter- tetrahedral bridging bonds in SiO_2[37] . The band at 1022 cm^{-1} corresponds to Si-O-Si stretching deformation[36]. Due to low loading of ZrO_2 over the clay surface, there is no appreciable change in the FTIR peaks of both native clay and ZrO-DKC.

Zero point charge (pH_{zpc})

The point of zero charge of edges (pH_{zpc}, edge) is a key parameter to characterise the charging behaviour of edges. Point of zero charge of edges is the *p*H where *p*H dependent charge at edges is zero[38]. The *p*H pzc, edge for ZrO-DKC was found to be 6.57 as shown in Fig.1(D). It indicated that the prepared ZrO-DKC has a positive surface charge below *p*H=6.57 and above this the surface charge becomes negative. The native potters' clay particles have a negative ζ at all studied *p*H as shown in the Fig 1(E). The negative zeta potentials are due to dominating effect of the structural charge[38]. When ZrO_2 particles were loaded on the clay surface the resulting ZrO-DKC has positive zeta potential. The possible reason is that when ZrO_2 particles were loaded on the clay, the

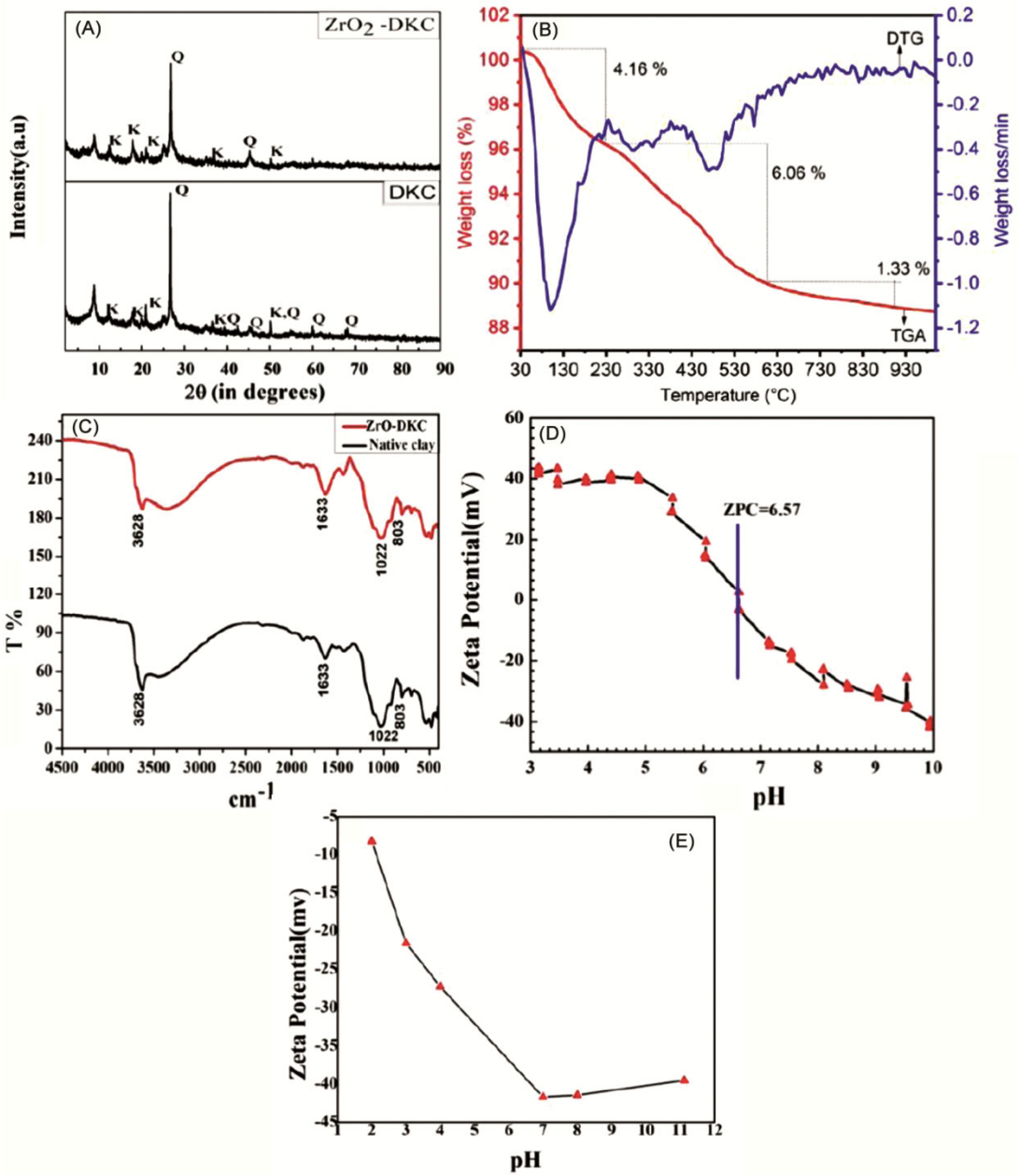

Fig. 1 — (A) Powder X-ray diffractrogram for oriented film of DKC & ZrO-DKC; (B) TG graph for ZrO-DKC; (C) FTIR pattern for DKC & ZrO-DKC; (D) Zeta-potential of ZrO-DKC at different *p*H level and (E) Zeta-potential of native potter's native potter's clay at different *p*H level.

Table 1 — Powder XRD peak assignments

d-Values (Å)	Assignments
7.12, 4.45, 4.25, 2.56, and 1.81	Kaolinite (K)
3.34, 2.45, 2.28, 2.12, 1.81, and 1.37	quartz (Q)

protonation of zirconium oxide at low *p*H imparts positive chrage on the surface. This indicated that the prepared ZrO-DKC has the prospect of its utility for adsorption of negatively charged species like fluoride and arsenate even at lower *p*H.

XPS study

XPS elemental analyses of the ZrO-DKC, before and after adsorption are shown in Fig. 2 (A), 2(B), 2(C), 2(D), 2. (E), respectively. Before fluoride adsorption, the peaks observed at 184.67 and 182.16 eV are due to the $Zr3d_{3/2}$ and $Zr3d_{5/2}$, respectively[39]. After adsorption, a new peak observed at 684.14 is due the F1s[39]. The intensities of Zr3d peaks at binding energies 184.67 and 182.16 are observed to be decrease after adsorption. This indicates the

possible involvement of Zr metal in the formation of metal fluoride complex ZrF_4. The Zr3d region at a binding energy of 182.16 eV is in good agreements with binding energy for Zr(IV) in ZrO_2 [40]. The strong growth of the F1s peak demonstrates the remarkable fluoride adsorption on the adsorbent ZrO-DKC.

Surface morphology of the adsorbent

The SEM images show the layered and flaky structures of native clay, The SEM images of ZrO-DKC, and ZrO-DKC after fluoride adsorption as depicted in Fig 3 (A-C) and its corresponding SEM-EDX images which were carried out to determine the chemical composition of all the samples are depicted in right side. On comparison of the SEM-EDX of native clay, ZrO-DKC, and ZrO-DKC after flouride adsorption, it is seen that there is loading of Zr in ZrO-DKC surface after activation and a peak for flourine is observed after adsorption of flouride on ZrO-DKC surface. The presence of

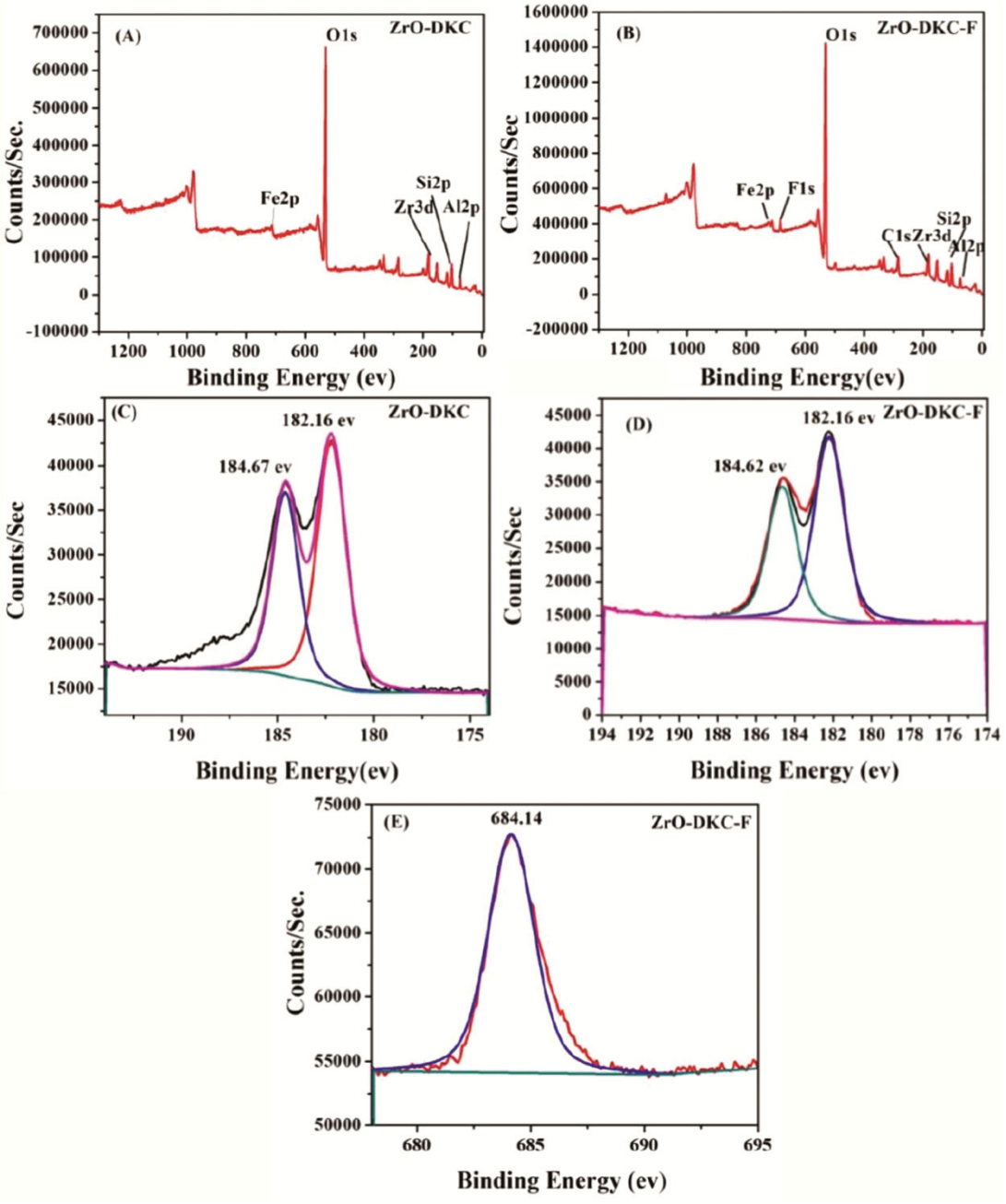

Fig. 2 — (A) Total XPS survey for ZrO-DKC before adsorption; (B) Total XPS survey spectra for ZrO-DKC after F^- adsorption; (C) Zr3d, before adsorption; (D) Zr3d, after adsorption and (E) F1s after adsorption on ZrO-DKC

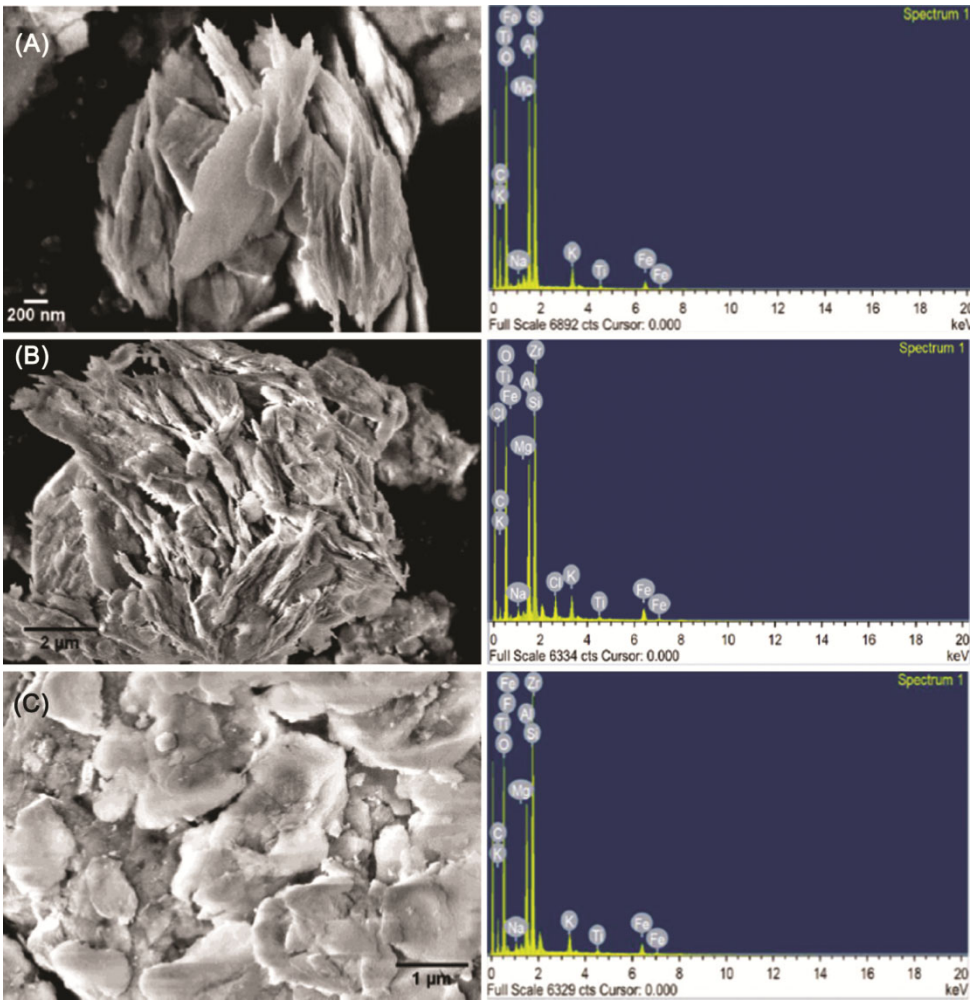

Fig. 3 — FESEM-EDX of (A) DKC; (B) ZrO-DKC and (C) ZrO-DKC after F^-adsorption

48.44 % oxygen indicates the other elements Al, Si, Ti, Fe, Zr are present as their oxides in ZrO-DKC[33]. The presence of 1.54 % Cl is due to addition of $ZrOCl_2.8H_2O$ to the system which was left as residue because of its trapping in the crystals during crystallization of zirconium oxide on the surface of clay. Presence of 0.7 % flourine on ZrO-DKC after flouride adsorption indicated that the material efficiently remove flouride from aqueous medium.

Surface area analysis (BET)

The BET surface area of ZrO-DKC, was found to be 44.147 m²/g with Pore Radius Dv(r) = 17.775 Å. The BET surface area of the raw clay was found to be 48.4 m^2/g with Pore Radius Dv(r)= 18.725 Å

Adsorbent dose study

From Fig. 4(A) it was observed that beyond 0.75 g of the adsorbent, there was no further increase of sorption efficiency, therefore 0.75 g was considered as optimum dose for this adsorption study. Remaining experiments were carried out by taking 0.75 g adsorbent per 20 mL F^- solution.

Effect of contact time

The results of the effect of contact time are plotted in Fig. 4(B). From the figure it is observed equilibrium was achieved at 120 minute contact time.

Kinetics study

Different kinetics models such as pseudo first order, pseudo second-order and Elovich rate equations were used to study the kinetics behaviour of adsorption of Fluoride onto the ZrO-DKC as shown in Fig.5 (A), (B), and (C), respectively (Table 2). Pseudo first-order model is the plot of log (q_e-q_t) versus t. The equilibrium sorption capacity, q_e, and first order rate constant can be known from the slope and intercept of the plot. High value of regression coefficient value

0.99 indicated the favourability of the model. Pseudo-second order model is represented by the linear plot of t/q_t versus t. the value of regression coefficient is almost unity (0.999), which indicated that the pseudo-second order model is suitable for fitting data. The plot of q_t versus lnt is related to Elovich model[41] which describes the diffusive nature of the adsorption process. On comparing the R^2 values of different kinetic models, pseudo second-order model is observed to be the most acceptable and finest fitted

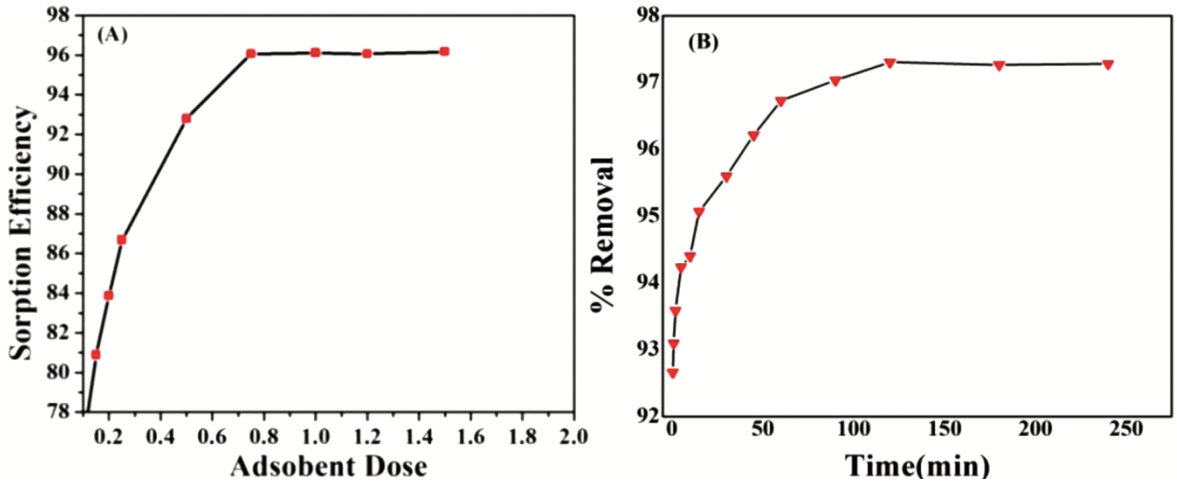

Fig. 4 — Effect of (A) adsorbent dose and (B) Contact time

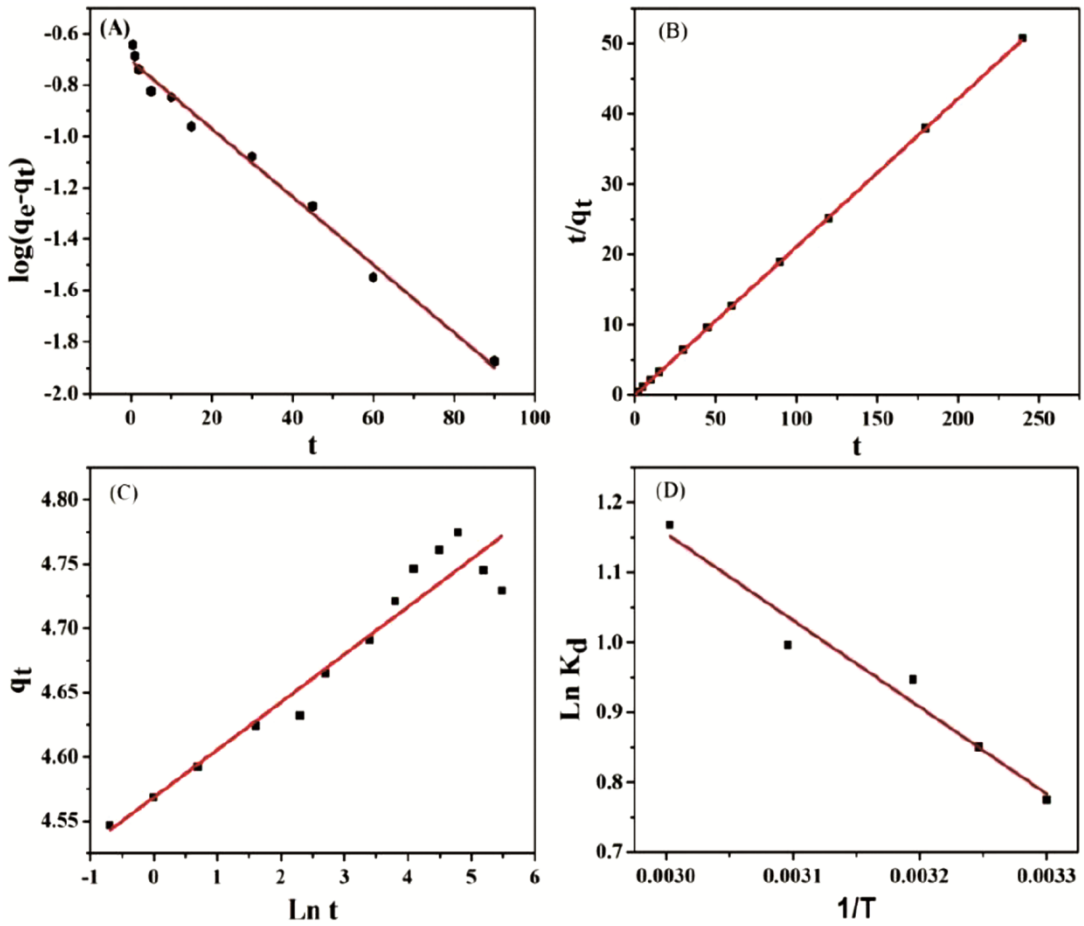

Fig. 5 — (A) Pseudo 1st order; (B) pseudo 2nd Order and (C) Elovich Kinetics Models

with $R^2 > 0.99$ for Zirconium oxide decorated potters clay (ZrO-DKC). The considerable fitting of Elovich model showed that pore diffusion plays a vital role in the rate of the reaction.

Table 2 — Comparison of pseudo first order, pseudo second order model rate constants and calculated q_e values

Kinetics models	Parameters	Value
(A) Pseudo First order	$K_1(min^{-1})$	0.03
$\log(q_e - q_t) = \log q_e - \frac{k_1}{2.303} t$	$q_{e,\,cal}$ (mg/g)	0.8504
	R^2	0.9876
(B) Pseudo Second order	$K_2(min^{-1})$	4.175
$\frac{t}{q_t} = \frac{1}{k_2 q_e^2} + \frac{t}{q_e}$	$q_{e,\,cal}$ (mg/g)	4.742
	R^2	0.99
(C) Elovich Model	b (g/mg)	27.03
$q_t = \frac{1}{b}\ln(a\,b) + \frac{1}{b}\ln t$	a (mg/(g min)	0.155
	R^2	0.9258

Adsorption isotherm study

In this study, three key isotherm models i.e. the Langmuir, Freundlich, Temkin, were utilized to learn about the adsorption behaviour of fluoride over finely ground ZrO-DKC at 30°C shown in Fig. 6(A), 6(B), and 6(C) respectively. The observed distinctive trial information is listed in Table 3. The plot of C_e/q_e versus C_e can be depicted as Langmuir isotherm. The slope and intercepts of the plots gives Langmuir Constant (K_L) and the theoretical monolayer adsorption capacity Q_o. From the plot Q_o was observed to be. 2.18 mg/g. The separation factor R_L, [1/ (1+K_L C_o)] explains the shape of the isotherm and adequacy of the Langmuir model to fit the information. Separation factor R_L is found to be less than unity, which suggested that the Langmuir model is suitable for fit the data in our study[41,42].

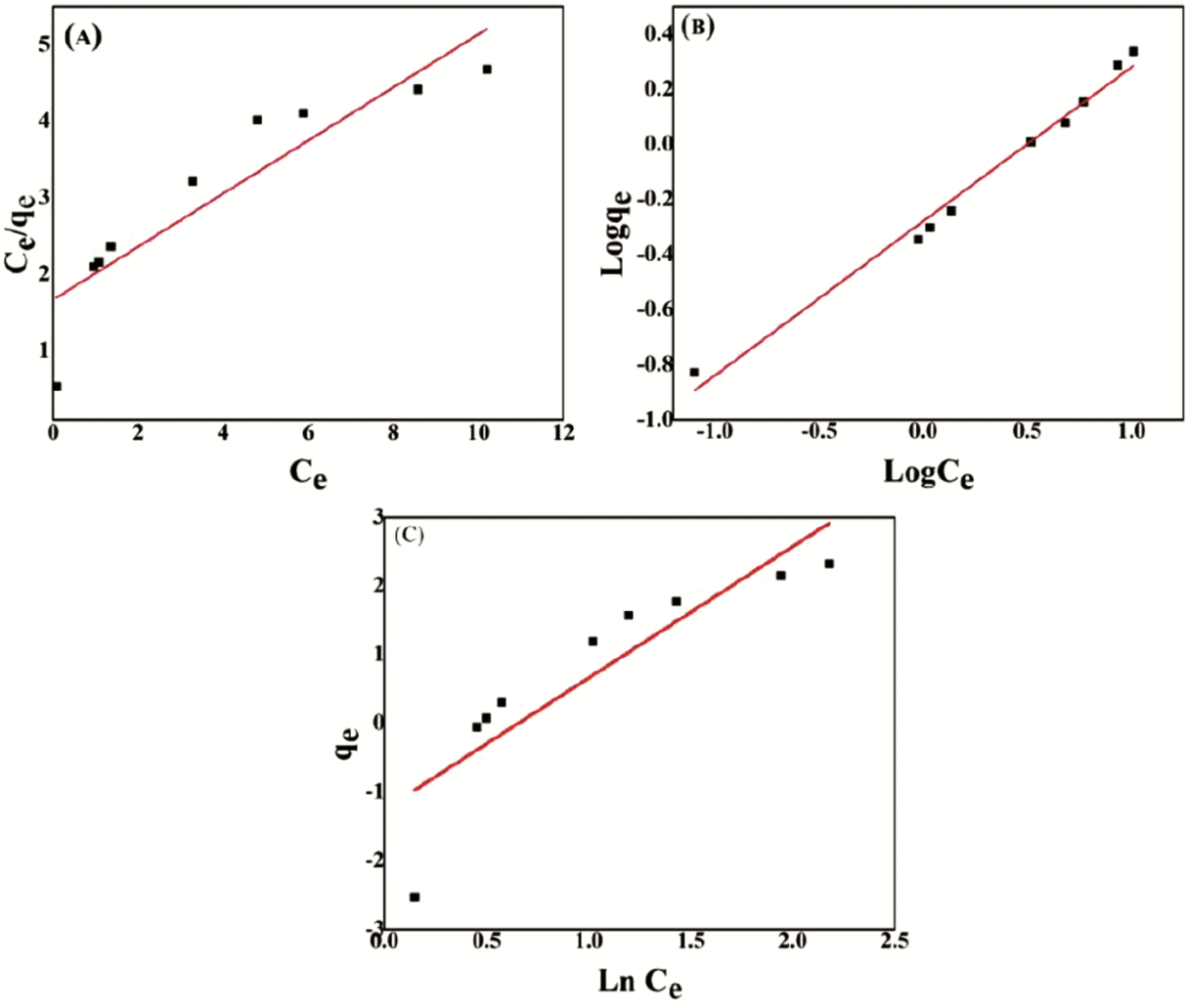

Fig. 6 — (A) Langmuir Adsorption Isotherm; (B) Freundlich Adsorption Isotherm; (C) Temkin Adsorption Isotherm and (D) Van't Hoff isotherm plot of fluoride adsorption.

Freundlich adsorption constant K_f, intensity of adsorption, and Freundlich constant (n), were calculated from the linear plot of $\log q_e$ versus $\log C_e$. If Freundlich constant (n) lies between 1 and 10, the adsorption of F^- is favourable on the adsorbent surface[44]. The high values of n and K_f signifies the effective uptake of F^- ion onto the ZrO-DKC adsorbent surface[40, 43] as shown in Table 3.

The Temkin isotherm is a plot of q_e versus $\ln C_e$ where A_T and B (RT/b_T) are Temkin constants and b_T is the Temkin constant correlated to heat of sorption (kJ/mol). The value of b_T (kJ/mol) derived from Temkin Isotherm was found to be 1.316 which indicated that the type of adsorption is physical in nature[41].On comparing the correlation coefficient values of the linear plot of the different models, Freundlich isotherm model was found to be the most suitable for F^- adsorption with $R^2>0.95$ for ZrO-DKC.

Adsorption thermodynamics

From the study of effect of temperature on adsorption, it was found that there was no any considerable change in the adsorption efficiency on increase in temperature. To evaluate different thermodynamic parameter Van't Hoff isotherm was plotted shown in Fig.6 (D). The ratio of q_e and C_e gave the adsorption equilibrium constant Kd[41, 45]. The slope and intercept of the plot of $\ln K_d$ versus 1/T gave adsorption enthalpy (ΔH^o) and adsorption entropy (ΔS^o), respectively[43]. Adsorption free energy was obtained from Gibbs isotherm equation [ΔG^o (-RT ln K_d)] and listed in Table 4. Generaly, the value of adsorption enthalpy (ΔH^o) for physical adsorption is observed to be below 40 kJ mol^{-1}. However, in this study, it is found to be 10.31kJ mol^{-1} which indicated that nature of the adsorption is physical adsorption[41]. The positive enthalpy value indicates that the adsorption process is endothermic in nature. Negative value of ΔG^o and positive value of ΔS^o signify the encouraging defluoridation capacity of ZrO-DKC surface[43].

Effect of co-existing anion

The effect of different co-existing anion on adsorption is shown in Fig.7 (A). From the figure it is seen that Cl^- and Br^- ions showed encouraging effect on fluoride adsorption[44] while SO_4^{2-}, CO_3^{2-}, and PO_4^{3-} have negative effect towards defluoridation efficiency of the adsorbents[44] .Figure 7(A) showed that the order of defloridation efficiency in the presence of co-existing anions is $CO_3^{2-} < SO_4^{2-} < Br^- \approx Cl^-$. Defluoridation efficiency in the absence of co-existing anions was 94.7%, which decreased to 93.8% in presence of SO_4^{2-}, 93.6% in presence of CO_3^{2-}, and to 91.5% in the presence of PO_4^{3-}. Moreover, in the presence of all the anions the defluoridation efficiency reduced to 90.4%. This decrease in adsorption efficiency is owing to the possible competition of different anions towards the adsorption site[16, 44].

Effect of pH

The effect of *p*H on adsorption is shown in Fig.7 (B). Efficiency of adsorption is observed to be dependent on *p*H of the solution. From the Fig. 7(B), it is obvious that efficiency of adsorption sharply increases at lower *p*H below *p*H ≈ 4 and decreases above *p*H ≈ 7. Fluoride removal efficiency increases in the acidic pH range which is due to the presence of positive sites and neutral sites on the surface of the adsorbent that facilitated for more fluoride ions to bind on the surface[16,47]. Decline of sorption efficiency in basic *p*H region may be is due to competition of hydroxide and fluoride ions for adsorption site[47] . When *p*H increases, number of hydroxyl ion in the solution increases. As OH^- and F^- has almost similar ionic radii so efficiency of adsorption decreases due to possible completion for surface adsorption site[4].

Table 3 — Comparison of Langmuir, Freundlich, Temkin isotherm constants, and correlation coefficients using ZrO-DKC

	Isotherm models	Parameters	Values
(A)	Langmuir isotherm $\frac{C_e}{q_e} = \frac{C_e}{Q_o} + \frac{1}{Q_o K_L}$	Q_0 (mg/g)	2.884
		K_L (L/mg)	0.207
		R_L	0.855
		R^2	0.80752
(B)	Freundlich isotherm $\log q_e = \log K_f + \frac{1}{n}\log C_e$	K_f (mg/g(L/mg)$^{1/n}$)	0.5272
		n	1.8
		R^2	0.9838
(C)	Tempkin isotherm $q_e = B \ln A_T + B \ln C_e$	A_T (L/g)	0.5204
		B (J/mol)	1.914
		b_T (kJ/mol)	1.316
		R^2	0.754

Table 4 — Different thermodynamics parameters

ΔH^o (KJ mol^{-1})	ΔS^o (KJ mol^{-1})	ΔG^o (KJ mol^{-1}) at different temperature				
		303 (K)	308(K)	313 (K)	323 (K)	333(K)
10.311	0.0405	-1.951	-2.176	-2.463	-2.674	-3.234

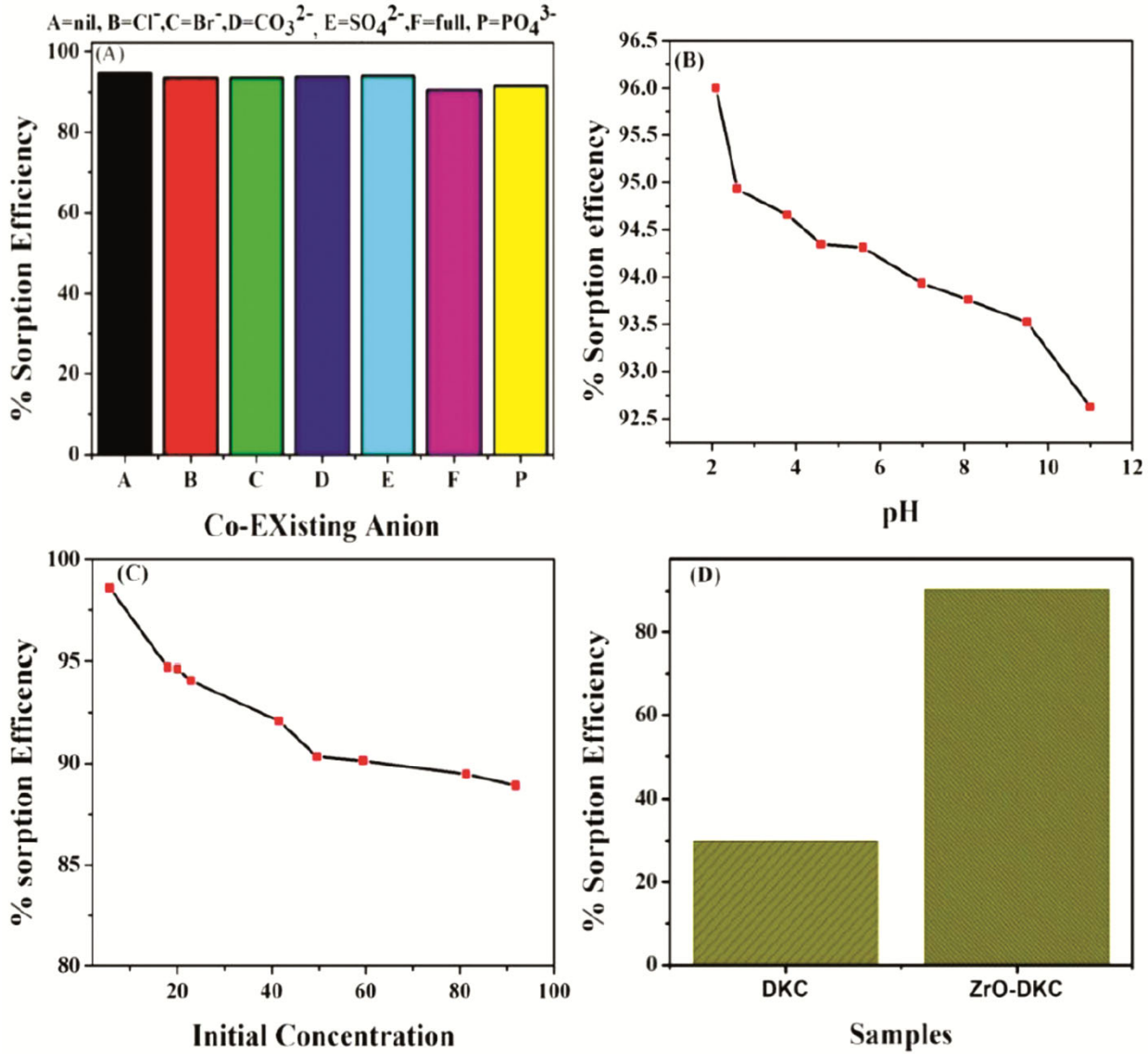

Fig. 7 — (A) Effect of co-existing anions on defluoridation; (B) Effect of *p*H on defluoridation; (C) Effect of initial concentration on sorption efficiency and (D) Comparison of Sorption Efficiency of native & activated clay (ZrO-DKC)

Effect of initial concentration

The effect of initial concentration on adsorption is as shown in Fig.7(C). Impact of increase in initial fluoride concentrations on the fluoride removal percentage at equilibrium is found to be less prominent which demonstrated that the material can be employed in wide fluoride concentration ranges. When the initial concentration decreases from 91.9 mg L^{-1} to 5.65 mg L^{-1}, the sorption efficiency is observed to be increases from 88.9% to 98.5%.

Field sample study

The different chemical parameters of the investigated groundwater are listed in Table 5. Due to the competing anions such as phosphate, sulphate and

Table 5 — Chemical composition of real life ground water.

Parameters	Value
*p*H	7.3
Sodium	34.346 mgL^{-1}
Potassium	1.718 mgL^{-1}
Calcium	13.699 mgL^{-1}
Magnesium	1.866 mgL^{-1}
Fluoride	4.257 mgL^{-1}
Bromide	0.808 mgL^{-1}
Chloride	1.773 mgL^{-1}
Phosphate	0.987 mgL^{-1}
Sulphate	0.277 mgL^{-1}
Bicarbonate	165 mgL^{-1}

Table 6 — Comparison between various reported adsorbents for fluoride removal.

Name of the adsorbent	Adsorption capacity (mg/g)	Reference
Red soil (Laterite)	0.5	49
Montmorillonite clay	0.26	50
Ceramic adsorbent	2.16	51
Hydrated cement	2.7	52
La(III) incorporated carboxylated chitosen bead	4.71	53
Fe-Al impregnated granular ceramic adsorbent	3.56	54
Alum bentonite	5.7	55
Acid activated Kaolinite clay	0.1	56
Activated alumina	1.1	57
Zirconium oxide mediated potters clay (ZrO-DKC)	2.18	Present work

bicarbonate present in the groundwater, defluoridation capacity decreases in comparison to the spiked water containing only Fluoride ion. The remaining concentration was decreased to 0.370 mg L^{-1} from 4.27 mg L^{-1} by ZrO-DKC using 37.5 g L^{-1}. Percentage removal in case of real life water was observed to be 91.33 whereas the same amount of adsorbent can remove fluoride from equally concentrated spiked water to below detectable limit i.e. more than 99.99%.

Comparison between the adsorption efficiency of raw clay and ZrO-DKC

A 50 mg L^{-1} fluoride spiked solution was prepared for the study. Equal amount (0.75 g) of native clay adsorbent and ZrO-DKC were taken and sorption efficiency was studied with 20 mL of 50 mg L^{-1} spiked fluoride solutions for 120 minutes. After adsorption on native potters clay the concentration came down to 35 mg L^{-1}, whereas for adsorption on activated potters' clay (ZrO-DKC) it came down to 4.8 mg L^{-1}. Efficiency increased from 30% to 90.4%. The results are shown in Fig.7 (D). A comparison between various reported adsorbents for fluoride removal is reported in Table 6.

Possible mechanism of adsorption

A possible mechanism of adsorption was studied and is proposed here. In an aqueous medium Zirconium is bonded to water or to water derived species like hydroxide or oxide. In reactions carried out in aqueous medium displacement of oxygen can happen from the zirconium-oxygen species by the formation of a stronger bond with a reactive species to occupy the position of the previously existing bond. This happens by the successive protonation of the oxygen attached to zirconium[48].

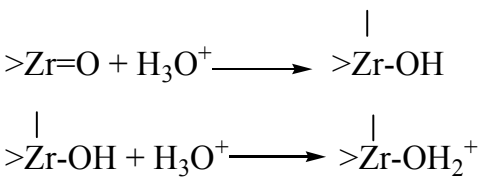

When medium becomes more acidic (pH <4), protonation of oxygen bound to zirconium occurs extensively. The protonated zirconium hydroxide forms a strong Columbic interaction with the fluoride anions present in the solution. Apart from that the protonated zirconium hydroxide also forms strong interaction with the negatively charged clay surface thereby making a composite site for adsorption of fluoride over Zr modified clay.

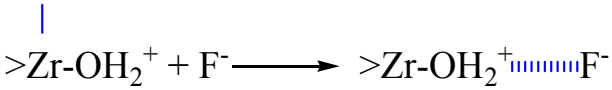

Conclusion

In the current study a low cost adsorbent by surface modifying locally available clay has been prepared and characterised. The performance of the prepared composite adsorbent towards removal of toxic fluoride has been studied. Impact of adsorbent dose, *p*H, contact time, temperature, and concentration of the adsorbates and effect of co-existing anions on adsorption are studied. Adsorption isotherms and adsorption kinetics are also studied. Positive values of ΔH^o and ΔS^o, and negative values of ΔG^o signifies the feasibility of the adsorption process. The prepared adsorbent is found to be very efficient in a wide pH range of 3-11. Its adsorption efficiency is very high even in the presence of competing anions. The adsorbent is based on naturally occurring clay material and due to its wide availability and environmental benignity, development of adsorbent

based on clay can be proposed as a better solution for fluoride removal and to provide safe water to the people residing in the fluoride endemic areas as these clay minerals are widely available in such areas.

Acknowledgements

The authors are thankful to the Director, CSIR-NEIST, Jorhat, India for allowing me to publish the work The authors are also thankful to Chemistry Department, Gauhati University, Assam, India for giving the opportunity to register under Ph. D programme.

References

1 Elhalil A, Qourzal S , Mahjoubi F Z , Elmoubarki R, Farnane M, Tounsadi H, Sadiq M, Abdennouri M & Barka N, *Emerg Contam*, 2 (2016) 42.
2 Goswami A & Purkait M K, *J Water Process Eng*, 1 (2014) 91.
3 Dhillon A, Nair M, Bhargava S K & Kumar D, *J Colloid Interface Sci*, 457 (2015) 289.
4 Wen S, Wang Y & Dong S, *RSC Advances*, 5 (2015) 89594.
5 Zhang J, Chen N, Tang Z, Yu Y, Hu Q & Feng C, *Phys Chem Chem Phy*, 17 (2015) 12041.
6 Amalraj A & Pius A, *Appl Water Sci*, 7 (2017) 2653.
7 Zhang K, Wu S, He J, Chen L, Cai X, Chen K , Li Y, Sun B, Lin D, Liu G, Kong L & Liu J, *J Colloid Interface Sci*, 475 (2016) 17.
8 Dong S & Wang Y, *Water Res*, 88 (2016) 852.
9 He J , Cai X , Chen K , Li Y , Zhang K , Jin Z , Meng F , Liuc N, Wang X , Kong L & Huang X, *J Colloid Interface Sci*, 484 (2016) 162.
10 Thathsara S K T, Cooray P L A T, Mudiyanselage T K, Kottegoda N & Ratnaweera D R, *J Environ Manage*, 207 (2018) 387.
11 Dessalegne M, Zewge F & Diaz I, *J Chem Technol Biotechnol*, l92 (2017) 605.
12 WHO, 2006, Fluoride in Drinking-water, London, UK .
13 Gomez-Hortigüela L, Perez-Pariente J, García R, Chebude Y & Diaz I, *Sep Purif Technol*, 120 (2013) 224.
14 Chen Y, Zhang Q, Chen L, Bai H & Li L, *J Mater Chem A*, 1 (2013) 13101.
15 Patil M M, Lakhkar B B & Patil S S, *Indian J Pediatr*, 85 (2018) 375.
16 Jagtap S, yenkie M K, Labhsetwar N & Rayalu S, *Chem Rev*, 112 (2012) 2454.
17 Jadhav S V, Bringas E, Yadav G D, Rathod V K, Ortiz I & Marathe KV, *J Environ Manage*, 162 (2015) 306.
18 Jin Z, Jia Y, Zhang K, Kong L, Sun B, Shen W, Meng F & Liu J, *J Alloy Compd*, 675 (2016) 292.
19 Shen J, Mkongo G, Abbt-Braun G, Ceppi S L, Richards B S & Schäfer AI, *Sep Purif Technol*, 149 (2015) 349.
20 Ansari M H, Parsa J B & Merati Z, *Chem Eng Res Des*, 126 (2017) 1.
21 Bhatnagar A, Kumar E & Sillanpaa M, *Chem Eng J*, 171 (2011) 811.
22 Ali I, Alothman Z & Sanagi M, *J Mol Liq*, 211 (2015) 457.
23 Tian Y, Wu M, Liu R, Wang D, Lin X, Liu W, Ma L, Li Y & Huang Y , *J Hazard Mater*, 185 (2011) 93.
24 Medellin-Castillo N A, Leyva-Ramos R, Ocampo-Perez R, Cruz R, Aragon-Pina A, Martinez-Rosales J, Guerrero-Coronado R & Fuentes-Rubio L, *Ind Eng Chem Res, 46 (2007) 9205.*
25 Maliyekkal S, Shukla S, Philip L & Nambi I, *Chem Eng J*, 140 (2008) 183.
26 Halder G, Sinha K & Dhawane S, *Desalin Water Treat*, 56 (2015) 953.
27 Ma W, Chen Y, Zhang W & Zhao W, *J Fluorine Chem*, 200 (2017) 153.
28 Bhattacharyya K G & Sen Gupta S, *Adv Colloid Interface Sci*, 140 (2008) 114.
29 Vinati A, Mahanty B & Behera S K, *Appl Clay Sci*, 114 (2015) 340.
30 Sarmah S, Saikia J, Bordoloi D & Goswamee R L, *J Environ Chem Eng*, 5 (2017) 4483.
31 McDaniel M P, *Adv Catal*, 53 (2010) 128.
32 Ntim S, Mitra S, *J Colloid Interface Sci*, 375 (2012) 154.
33 https://en.wikipedia.org/wiki/Zirconium Access on 07/12/18
34 https://www.lenntech.com/periodic/elements/zr.htm.Access on 07/12/18
35 Chaudhry S A, Khan T A & Ali I, *Egypt J Pet*, 26 (2017) 553.
36 Angaji M T, Zinali A Z & Qazvini N T, *WJNSE*, 3 (2013) 161.
37 Saikia B J & Parthasarathy G, *J Mod Phys*, 1 (2010) 206.
38 Pecini E M & Avena M J, *Langmuir*, 29 (2013) 14926.
39 Dou X, Mohan D, Pittman C U & Yang S, *Chem Eng J*, 198 (2012) 236.
40 Zhang J, Chen N, Su P, Li M & Feng C, *React Funct Polym*, 114 (2017) 127.
41 Saikia J, Sarmah S, Ahmed T H, Kalita P J & Goswamee R L, *J Environ Chem Eng*, 5 (2017) 2488.
42 Ahire M & Bhagwat S, *Indian J Chem Technol*, 26 (2019) 23.
43 Rangabhashiyam S, Sujata L & Balasubramanian P, *Surf Interfaces*, 10 (2018) 197.
44 Gogoi C, Saikia J , Sarmah S, Sinha D & Goswamee R L, *Water Air Soil Pollut*, 229 (2018) 118.
45 Gao C , Yu X Y , Luo T , Jia Y , Sun B , Liu J H & Huang X J, *J Mater Chem A*, 2 (2014) 2119.
46 Shen J, Evangelista M, Mkoongo G, Wen H, Langfor R, Rosair G, McCoustra M & Arrighi V, *Adsorption*, 2 (2018) 135.
47 Alemu S, Mulugeta E, Zewge F & Chandravanshi B S, *Environ Technol*, 35 (2014) 1893.
48 Blumenthal W B, *Talanta*, 8 (1968) 877.
49 Bjorvatn K, Bardsen A & Haimanot R T, *Desalination*, 201 (2006) 267.
50 Chen N, Zhang Z, Feng C, Sugiura N, Li M, Zhu D, Chen R & Sugiura N, J Hazard Mater, 183 (2010) 460.
51 Kagne S, Jagtap S, Dhawade P, Kamble S P, Devotta S & Rayalu S S, *J Hazard Mater*, 154 (2008) 88.
52 Viswanathan N & Meenakshi S, *J Colloid Interface Sci*, 322 (2008) 375.
53 Chen N, Feng C & Li M, *Clean Techno Environ Policy*, 16 (2014) 609.
54 Vhahangwele M, Mugera G W & Tholiso N, *Toxicol Environ Chem*, 96 (2014) 1294.
55 Gogoi P K & R Baruah, *Indian J Chem Technol*, 15 (2008) 500.
56 Maliyekkal S M, Sharma A K & Philip L, *Water Research*, 40 (2006) 3497.